Liquid−Vapor Phase Equilibria and Surface Tension of Ethane As Predicted by the TraPPE and OPLS Models†

Jorge Benet, Luis G. MacDowell,* and Carlos Menduiña

Departamento de Química Física, Facultad de Ciencias Químicas, Universidad Complutense de Madrid, 28040, Spain

In this work we combine two recently proposed computer simulation techniques: the wandering interface method for the calculation of surface tensions and Janecek's method for the estimation of long-range dispersive interactions to predict the surface tension of ethane. We have obtained results for two well-known models, the transferable potentials for phase equilibria (TraPPE) and optimized potentials for liquid simulations (OPLS) force fields. We show that neglecting long-range contributions to the dispersive energy as it is often done may yield surface tensions that are far too low by as much as 40 %. Such contributions can be effectively accounted for, however, and the resulting liquid−vapor coexistence densities and surface tensions show a rather good agreement for the TraPPE model, but quite less so for the OPLS model.

Introduction

Despite enormous activity during decades, there remains an ongoing research effort on the measurement of liquid−vapor coexistence properties. Together with careful measurements and progress in instrumentation, there is the need for developing less expensive albeit reliable tools for correlation and prediction. In Paris in 1982 and 1983 one of us enjoyed the opportunity of testing and developing correlations to our own experimental data in the company of Professor Kehiaian. At that time, computer simulations were just a promising tool with few practitioners, but it has clearly become nowadays the method of choice in many situations, as they have shown to have predictive value at a modest computational cost.[1]

Whereas the calculation of coexistence properties by computer simulations is an almost routine task nowadays,[2−4] the situation is not quite the same as regards the calculation of surface tensions. The reason is that coexistence properties may be obtained reliably by simulating bulk liquid and vapor phases without the need to explicitly consider an interface, with techniques such as the Gibbs ensemble simulation method and the NpT + test particle methods.[5,6] On the other hand, it is obviously not possible to calculate the surface tension without explicit simulation of the vapor−liquid interface. This implies a number of complications that are only recently being dealt with satisfactorily.

First of all, the need for simulating an interface explicitly requires usually fairly large systems, since both the liquid and the vapor phases need to be simulated, as well as the interface. Such simulations are therefore quite computer-demanding relative to bulk simulations. Furthermore, system size effects appear that need careful assessment. The size of the systems can no longer be described by the mere number of molecules. Also, the lateral size and perpendicular distance to the interphase become relevant variables. Too small a surface area is known to produce unreliable results, as reflected by an oscillatory dependence of the surface tension on the lateral size.[7,8] Too small a perpendicular distance to the interphase does not properly allow for the coexisting phases to adopt the corresponding asymptotic bulk regime.

Another important issue that has received much attention in the past few years is the way to extend the well-known long-range corrections of the intermolecular potential for systems with an inherent inhomogeneous density profile.[9−14] Whereas for bulk fluids such corrections are a trivial matter,[15] the development of correct expressions allowing to account for the inhomogeneous density profile has been a matter of discussion for a long time.[16−18]

However, not only are these technical issues a matter of concern. Even the basic statistical mechanical expression for the calculation of surface tensions has been a controversial issue over the years,[19] with several different expressions proposed for the pressure tensor.[20−22] It is now well-understood that these apparently different expressions for the virial yield the same values of the surface tension upon integration. However, the correct calculation of the components of the pressure tensor remain a challenging task for complex molecular fluids, particularly if the model includes constraints such as fixed bond lengths or angles.[23] For this reason, there has been a renewed interest in finding efficient methodologies for the calculation of the surface tension which do not require explicitly the calculation of the pressure tensor.[24−26]

A promising method that was shown to yield accurate results for the surface tension of model polymers is known as the wandering interface method (WIM).[17,26,27] In this method the coexisting phases are placed inside an elongated prismatic box, and the surface area of the system is allowed to fluctuate randomly. The extent of the fluctuations is dictated by the surface tension, which can be estimated from the study of such fluctuations. This method has a number of advantages, since there is no need for explicit evaluation of the pressure tensor, and the method may be applied to bound (fluid−solid) or free (liquid−vapor) interfaces alike. Furthermore, this method allows an easy implementation of long-range corrections for inhomogeneous fluids as those proposed recently by Janecek.[9]

In this work we use WIM in combination with Janecek's method for the calculation of long-range corrections to asses the quality of two of the most well-known united atom models

† Part of the "Workshop in Memory of Henry V. Kehiaian".

* To whom correspondence should be addressed: E-mail: luis@ender.quim.ucm.es.

10.1021/je100578z
Published on Web 08/25/2010

Table 1. Model Parameters for the Force Fields Employed in This Work

model	united atom	(ε/k_B)/K	σ/Å	l/Å
TraPPE	ethane CH_3	98.0	3.75	1.54
OPLS	ethane CH_3	104.1	3.775	1.53

for ethane, the transferable potentials for phase equilibria (TraPPE) and optimized potentials for liquid simulations (OPLS) models.[28,29]

Model and Simulations

Molecular Model. We describe ethane using a united model approach, whereby the CH_3 groups of the molecule are lumped into a single interaction site of the Lennard−Jones type:

$$u^{LJ}(r_{ij}) = 4\varepsilon_{ij}\left[\left(\frac{\sigma_{ij}}{r_{ij}}\right)^{12} - \left(\frac{\sigma_{ij}}{r_{ij}}\right)^{6}\right] \quad (1)$$

In this way, ethane is modeled effectively as a dimer with fixed bond length, l. The molecular parameters that need to be fit for agreement with experimental properties are ε, σ, and the bond length. In this work we have employed two well-known parametrizations for hydrocarbons, the TraPPE and the OPLS models. The actual choice of parameters for these models may be found in Table 1.

Surface Tension. The computation of the surface tension is carried out using the WIM method. The WIM technique is an extension of the *NpT* ensemble in which the interfacial area, A, is allowed to fluctuate at random. This is achieved by introducing a new Monte Carlo (MC) move, which consists of an attempt to deform the box by changing the interfacial area of the system at constant volume. The attempted moves are accepted according to the usual canonical rules, and the surface tension may be extracted from the resulting surface area probability distribution. Indeed, it can be shown that the free energy of an NVT (constant number volume and temperature) system with a given value of interfacial area is given by:[26]

$$F(A) = -k_B T \ln P(A) \quad (2)$$

where $P(A)$ is the probability of finding the system with area A and k_B is Boltzmann's constant. Identifying the macroscopic free energy of the coexisting states with γA, we find immediately the working expression for WIM:

$$\ln P(A) = -\frac{\gamma}{k_B T}A + C \quad (3)$$

where C is an irrelevant constant. Accordingly, we set up a simulation box with a tetragonal shape, having a liquid slab in the middle surrounded by two vapor phases at each side. The vapor−liquid interface is sampled as in an ordinary NVT ensemble, but once in a while we attempt to change the box shape by changing the lateral size while keeping the volume constant. Such moves are accepted with the usual probability rule of canonical simulations, that is, with probability given by the ratio of Boltzmann factors before and after the attempted move. During the course of the simulation a histogram of interfacial areas is collected. At the end of the simulation, we plot ln $P(A)$ against A and perform a linear fit of the data. The slope of the fit yields readily the surface tension, and the standard error of the slope yields a 68 % confidence estimate of the uncertainty. Since the surface tension is positive, the system will gradually elongate so as to reduce the surface are as much as possible. To avoid too-stretched simulation boxes, which would produce incorrect results, we simply bracket the interval of sampling within appropriate limits. Note that for the special case of discrete sampling of the surface area, the WIM technique becomes equivalent to the recently expanded ensemble methodology.[30,31]

Long-Range Corrections. Recent studies have shown that neglecting interactions beyond the cutoff distance may result in a very significant decrease of the surface tension, by an amount which can well reach 40 % at moderate temperatures.[9,17] For that reason, we need to consider a procedure for effectively summing up interactions beyond a cutoff.

In practice, the energy felt by species i due to interactions beyond the cutoff distance may be expressed in terms of the instantaneous density profile as:

$$U_i^{lrc} = \int_{V \ni \mathcal{S}(R_c, r_i)} \rho(\mathbf{r}) u(\mathbf{r}_i, \mathbf{r})\, d\mathbf{r} \quad (4)$$

where R_c is the cutoff radius, $u(\mathbf{r}_i, \mathbf{r})$ is the intermolecular potential between two molecules located at $\mathbf{r}_i$ and $\mathbf{r}$, respectively, $\rho(\mathbf{r})$ is the number density at $\mathbf{r}$, and $\mathcal{S}(R_c, \mathbf{r}_i)$ is a sphere of radius R_c centered in $\mathbf{r}_i$. In a mean field sense the density profile is a function of z only, so that the volume integration is best performed as a sum over parallel slabs:

$$U_i^{lrc} = \int_{-\infty}^{\infty} \rho(z)\{\int_{A \ni \mathcal{C}(r_{||}^{min}, z_i)} u(\mathbf{r}_i, \mathbf{r}) d\mathbf{r}_{||}\} dz \quad (5)$$

where $\mathcal{C}(r_{||}^{min}, z_i)$ is a circle of radius $r_{||}^{min}$ centered at z_i. $r_{||}^{min} = (R_c^2 - (z - z_i)^2)^{1/2}$ for $R_c^2 > (z - z_i)^2$ and zero otherwise.

For the special case of the Lennard−Jones potential, the term in brackets may be integrated right away using cylindrical coordinates, leading to:

$$U_i^{lrc} = \int_{-\infty}^{\infty} \rho(z) w(z - z_i)\, dz \quad (6)$$

with

$$w(z) = \begin{cases} 4\pi\sigma^2\varepsilon\left[\frac{1}{5}\left(\frac{\sigma}{R_c}\right)^{10} - \frac{1}{2}\left(\frac{\sigma}{R_c}\right)^{4}\right] & z \le R_c \\ 4\pi\sigma^2\varepsilon\left[\frac{1}{5}\left(\frac{\sigma}{z}\right)^{10} - \frac{1}{2}\left(\frac{\sigma}{z}\right)^{4}\right] & z > R_c \end{cases} \quad (7)$$

where σ and ε are the units of distance and energy of the Lennard−Jones intermolecular potential, respectively. The above equation is the long-range correction for the internal energy obtained by Janeček.[9] The result includes nonvanishing contributions for slabs at distances less than R_c, which were implicitly neglected in the corrections to the force previously employed by Mecke et al.[17,32]

The total energy arising from long-range corrections is given as a sum over individual contributions, with a factor of 1/2 not to include mutual interactions twice:

$$U^{lrc} = \frac{1}{2}\sum_{i=1}^{N} \int_{-\infty}^{\infty} \rho(z) w(z - z_i)\, dz \quad (8)$$

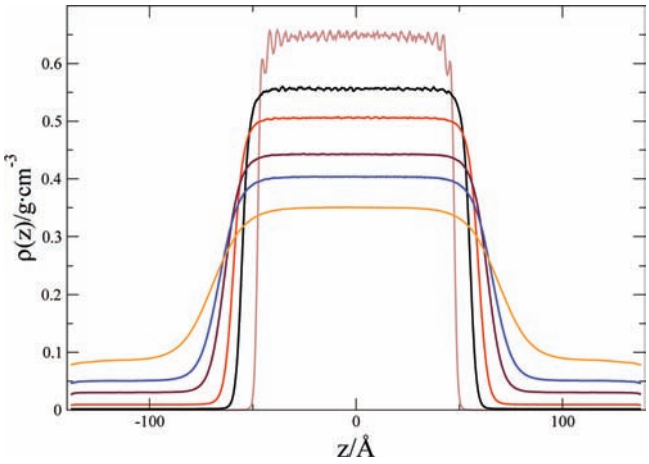

Figure 1. Simulated density profiles as obtained for the TraPPE model at several temperatures. The local density profiles are represented as a function of the perpendicular distance to the interface, with the origin placed at the system's center of mass. Note the liquid slabs at the center surrounded by vapor phases on each side. In order of decreasing liquid densities, results are for T = (100, 175, 213, 252, 271, and 290) K.

The above expression may be evaluated by discretization of the z coordinate and evaluation of the density inside slices centered at nodes z_k.[9,11,13,33]

Whereas the effective potential (c.f. eq 7) remains long-range and needs to be evaluated for all perpendicular distances within the simulation box, it is a more effective procedure than explicitly evaluating all pair interactions. Our own calculations show that using these long-range corrections with $R_c = 3\sigma$ is about as fast as truncation of the potential at $R_c = 4\sigma$.[14] Furthermore, it should be noted that the full long-range behavior cannot be simply recovered by increasing R_c to 6 or 8 molecular diameters, because the minimum lateral dimension must be $L_x = 2R_c$. As a result, a very large number of particles would be required to properly build a liquid slab.

Simulation Setup. Simulations are performed in the NVT ensemble with an MC code. We consider a system of $N = 1800$ molecules at a temperature T in a volume $V = L_xL_yL_z$, where L_x, L_y, and L_z are the dimensions of the rectangular simulation box. A homogeneous liquid system under periodic boundary conditions is first equilibrated in a cubic simulation box of dimensions $L_x = L_y = L_z \approx 10\sigma$. The simulation box is then expanded to $L_z \approx 72\sigma$ while keeping the lateral size constant and further equilibrated until well-defined vapor and liquid phases have developed.

Our code has been previously tested for agreement with the square well fluid,[34] the Lennard−Jones fluid,[35] and bead−spring Lennard−Jones chains,[24] among others.

All simulations are organized in cycles, where each cycle corresponds to N trial MC moves. Our MC procedure comprises three types of configurational updates: random displacement of the molecular center of mass, random rotation about a randomly chosen axis, and complete molecular regrowth of the molecules following the laws of configurational bias.[36,37] Within a cycle the three types of attempts are chosen randomly in the ratio 25:25:50. At the end of each cycle, a box deformation at constant volume is attempted. Explicit interactions between molecular sites are evaluated within a sphere with $R_c = 2.5\sigma$, while interactions beyond the cutoff are implicitly evaluated using the method described above. The vapor−liquid coexisting states are equilibrated for a period of $5 \cdot 10^5$ cycles, and results are collected for another $1 \cdot 10^6$ cycles. Further details of our computational procedure may be found elsewhere.[14,27,38]

Results

During the course of the simulation, density profiles $\rho(z)$ along the perpendicular distance to the interface, z, are measured. Figure 1 displays the results obtained for ethane as described by the TraPPE model for temperatures ranging from $T = 100$ K, close to the triple point, to $T = 290$ K, close to the critical point. All of the profiles clearly display a well-developed bulk liquid phase in the middle of the prismatic simulation box coexisting with vapor phases at both sides. Note that the liquid's slab position undergoes a random walk within the simulation box due to thermal agitation. Therefore, care must be taken to measure such profiles relative to the system's center of mass. Otherwise, the resulting density profile would gradually smoothen, and the information on the coexistence densities would wash away. Also note the rough structure of the density profile for the lowest temperature, $T = 100$ K. Such structure reveals strong correlations that are established across the interface and that need extremely long simulation times to smooth out.

Measuring the asymptotic densities at the liquid and vapor phases provides the information that is required to obtain the coexistence curve. The coexisting densities are estimated as the average value of the density profile within the region of asymptotic bulk densities. The uncertainties are estimated as one standard deviation of the mean. The results obtained in this work for the TraPPE and OPLS models are shown in Table 2. Figure 2 compares the results with experimental data,[39] as well as with previous simulations for a modified TraPPE model.[10,40] This is a TraPPE model with flexible (instead of rigid) bond length which we will henceforth name TraPPE_f (we feel this notation is more consistent than that used by Alejandre et al., who used TraPPE_UA instead). It is modified essentially for the purpose of using it in a molecular dynamics program without the need of including bond length constraints. The flexibility is incor-

Table 2. Coexistence Densities as Calculated in This Work for the TraPPE and OPLS Models and Comparison with Experimental Data from Ref 39[a]

	ρ_l/g·cm^{-3}				ρ_v/g·cm^{-3}			
T/K	TraPPE	OPLS	TraPPE_f	expt	TraPPE	OPLS	TraPPE_f	expt
100.0	0.648_4	0.646_7	-	0.6412	$1.3_6 \cdot 10^{-6}$	$1.5_6 \cdot 10^{-6}$	-	$4.0 \cdot 10^{-7}$
175.0	0.556_1	0.562_2	-	0.5558	0.00190_2	0.00100_2	-	0.0012
175.4	-	-	0.5532	0.5553	-	-	0.0013	0.0013
213.0	0.5058_5	0.5175_8	-	0.5061	0.00933_5	0.00552_3	-	0.0070
213.8	-	-	0.5016	0.5050	-	-	0.0060	0.0072
252.0	0.4426_3	0.4644_3	-	0.4442	0.0304_1	0.01880_8	-	0.0251
252.2	-	-	0.4386	0.4439	-	-	0.0208	0.0253
271.0	0.4034_3	0.4339_3	0.4049	0.4056	0.0507_1	0.0311_1	0.0376	0.0435
290.0	0.3502_3	0.3977_3	-	0.3517	0.0863_7	0.0499_1	-	0.0774

[a] Results are also shown for the TraPPE_f model.[10] The subscripts are uncertainties as given by one standard deviation of the mean (the order of magnitude being coincident with that of the last digit of the corresponding simulated value).

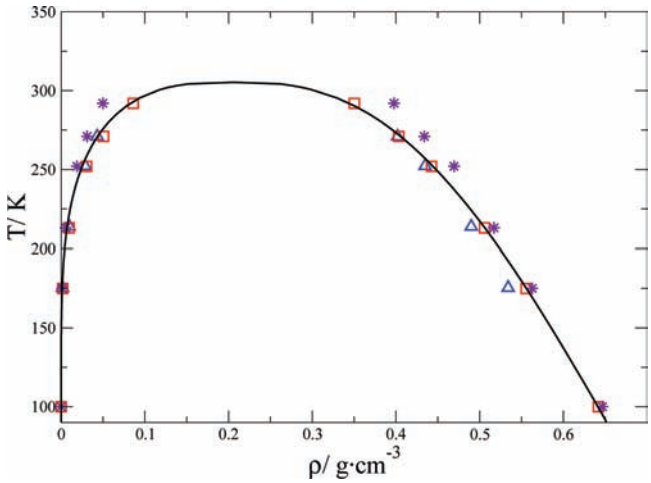

Figure 2. Coexistence densities for ethane as measured by the TraPPE (squares), OPLS (asterisk), and TraPPE_f (triangle) models compared with experimental results.[39]

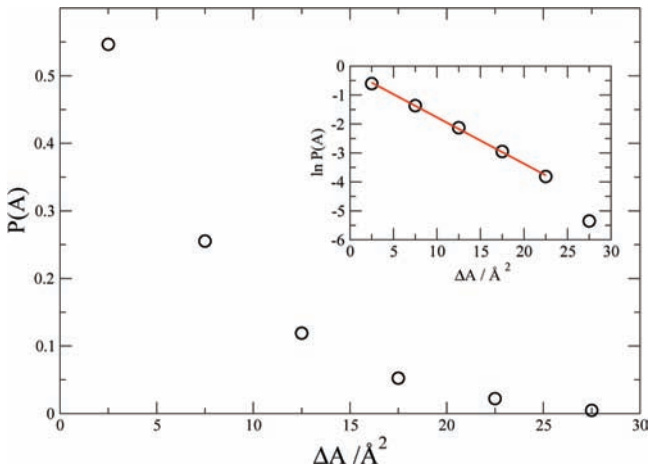

Figure 3. Interface area distribution as obtained for the TraPPE model at $T = 175$ K. The interface area is allowed to fluctuate between a minimum value of (38.25 Å)^2 and a maximum value of (38.60 Å)^2. $P(A)$ denotes the interface area probability and ΔA the interface area increment as measured from the minimum allowed value. The inset shows the result in logarithmic scale. The symbols are simulation results, and the straight line is a linear fit whose slope yields right away the surface tension (c.f., eq 3). Note the last point with large uncertainty is discarded from the fit.

porated by imposing a simple harmonic potential between adjacent sites, with an elastic constant of $k = 452,900$ K/Å^2.

Clearly, the TraPPE model shows excellent agreement for vapor and liquid coexistence densities in the temperature range studied. The TraPPE_f model, on the contrary, is somewhat less accurate predicting the bubble-point densities, particularly at low temperature. Finally, the OPLS model is seen to perform far less well than the TraPPE model, particularly for temperatures above 200 K.

The surface tensions may be obtained from inspection of the interfacial area probability distribution, as described by eq 3. Figure 3 shows $P(A)$ as obtained for the TraPPE model at $T = 175$ K. The symbols show a fast seemingly exponential decay that is dictated by the system's surface tension. The inset shows ln $P(A)$, where a clear linear behavior down to large area increments is demonstrated. Points corresponding to large area increments are very unlikely due to the exponential suppression of the probability. As a result, the last point does not quite follow the expected linear behavior due to poor sampling. Nevertheless, one can obtain a reliable least-squares fit from the remaining set of points and extract the surface tension from the slope $p = -\beta\gamma$.

Table 3. Surface Tension of Ethane as Predicted by the TraPPE and OPLS Models and Comparison with Experimental Results from Ref 39[a]

	γ/mN·m^{-1}			
T/K	TraPPE	OPLS	TraPPE_f	experiment
100	$33._1$	$36._1$	-	30.04
175	19.3_5	$22._1$	18.0_6	17.58
213	12.2_3	16.7_5	11.6_7	11.57
252	6.1_3	9.7_4	5.6_7	5.88
271	3.7_2	7.3_2	3.6_9	3.40
290	1.8_2	4.2_2	-	1.24

[a] Also included are predictions for the TraPPE_f model from ref 40. The subscripts are uncertainties as given by one standard deviation of the mean (the order of magnitude being coincident with that of the last digit of the corresponding simulated value).

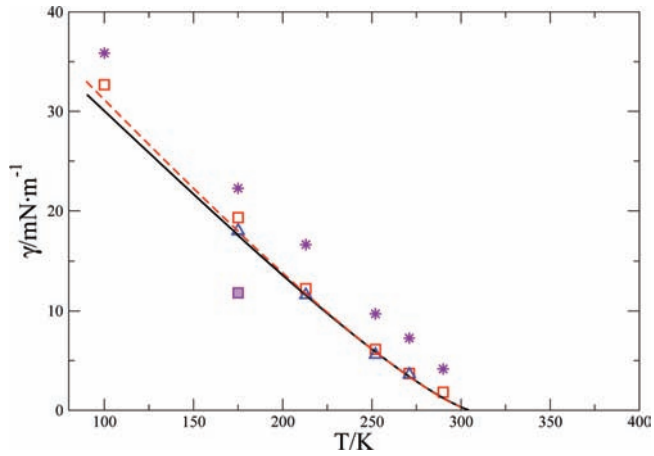

Figure 4. Surface tension for ethane as measured by the TraPPE (squares), OPLS (asterisks), and TraPPE_f (triangles) models compared with experimental results from ref 39 (continuous black line) and ref 41 (dashed red line). The shaded square indicates results for the TraPPE model with no long-range corrections.

The results obtained for the surface tension of ethane as predicted by the TraPPE and OPLS models are collected in Table 3, together with predictions from the TraPPE_f model and experimental results from ref 39. These same results are plotted in Figure 4, which also include experimental data from ref 41. Both experimental data sets agree nicely from the critical point down to $T = 175$ K, but clearly deviate below that temperature, with the NIST values somewhat below those of Baidakov. Such disagreement is not quite surprising considering the difficulty of the measurements. As to the different ethane models, we find the TraPPE and TraPPE_f models produce fair predictions, with the TraPPE_f model giving somewhat better results. This agreement is quite noteworthy, considering the fairly large temperature interval that we have studied, which spans the whole temperature range of the liquid phase. Note that the discrepancy between the model and the experimental results at low temperature is actually not larger than the discrepancy between different experimental results. Contrary to the good predictions of the TraPPE family, it is clear that the OPLS model is far less good at predicting the surface tension, largely overestimating the experimental results along the whole temperature range. This is not surprising, given that the OPLS model seems to be overestimating the critical temperature too.

It is noteworthy that neither the TraPPE nor the OPLS models were fit to surface tension data, so they may be considered as

predicting tools in this context. Thus, the better agreement of TraPPE might result from a better strategy for model parameter fitting in simulations. The OPLS model was mainly fitted to describe enthalpies of vaporization, while the TraPPE model was fitted for agreement with coexistence densities. Whereas both methodologies imply somehow fitting to coexistence properties, the OPLS parameters were fit at the time without a precise knowledge of the model's phase diagram, which makes the fitting procedure less reliable. On the contrary, the parameters from the TraPPE model were fit to precise liquid−vapor coexistence data obtained with the Gibbs ensemble method.[1]

Another important point to stress is the very large role the long-range corrections have in the calculated value of the surface tension. Figure 4 shows as a square the value that is obtained for the surface tension of the TraPPE model at $T = 175$ K when long-range corrections are neglected beyond a cutoff distance of $R_c = 9.375$ Å ($\approx 2.5\sigma$). The result obtained, $\gamma = 11.81$ mN·m^{-1}, is just 61 % of the value obtained when full long-range corrections are included, thus showing the importance of such corrections. On the other hand, considering that the TraPPE model yields quite good results for the coexistence densities but somewhat overestimates the surface tension, it might well be that the full long-range corrections could be somewhat larger than required. Note that, for long distances, the r^{-6} term of the dispersion forces is believed to gradually cross over to a somewhat faster decay of r^{-7} due to retardation effects of the electromagnetic field.[42] It is therefore not unexpected that integrating the r^{-6} all of the way to infinity could somewhat overestimate the surface tension.

Conclusions

In the present work we have calculated the surface tension of ethane for the TraPPE and OPLS force fields by means of computer simulations. We have shown that properly including dispersion interactions beyond a finite cutoff a few molecular diameters in length may account for as much as 40 % of the full surface tension. A slice by slice summation method proposed recently by Janecek is an efficient procedure for taking into account such contributions. This technique may be combined easily with the WIM for the calculation of surface free energies.[26]

Our results show that the TraPPE model produces a much better description of ethane's phase diagram than the OPLS model. The latter seems to incorrectly predict the coexistence properties close to the critical point and yields much too high surface tensions. The TraPPE model predicts the phase coexistence of ethane in rather good agreement, overperforming the modified TraPPE_f model. On the contrary, the TraPPE_f model predicts surface tensions in better agreement with the experiment. This shows the difficulty of finding a model that produces good results for several different properties. Further effort in model prediction of substances as simple as ethane is still required.

Acknowledgment

We would like to acknowledge helpful discussions with F. J. Blas.

Literature Cited

(1) Frenkel, D.; Smit, B. *Understanding Molecular Simulation*, 2nd ed.; Academic Press: San Diego, 2002.
(2) Mognetti, B. M.; Yelash, L.; Virnau, P.; Paul, W.; Binder, K.; Mueller, M.; MacDowell, L. G. Coarse Grained Models for Fluids and their Mixtures: Comparison of Monte Carlo Studies of their Phase Behavior with Perturbation Theory and Experiment. *J. Chem. Phys.* **2009**, *130*, 044101.
(3) Mognetti, B. M.; Virnau, P.; Yelash, L.; Paul, W.; Binder, K.; Mueller, M.; MacDowell, L. G. Coarse-graining dipolar interactions in simple fluids and polymer solutions: Monte Carlo studies of the phase behavior. *Phys. Chem. Chem. Phys.* **2009**, *11*, 1923–1933.
(4) Vrabec, J.; Huang, Y.-L.; Hasse, H. Molecular Models for 267 Binary Mixtures Validated by Vapor-Liquid Equilibria: A Systematic Approach. *Fluid Phase Equilib.* **2009**, *279*, 120–135.
(5) Panagiotopoulos, A. Z. Direct Determination of Phase Coexistence Properties of Fluids by Monte Carlo Simulation in a New Ensemble. *Mol. Phys.* **1987**, *61*, 813–826.
(6) Lotfi, A.; Vrabec, J.; Fischer, J. Vapour Liquid Equilibria of the Lennard-Jones Fluid from the NpT + Test PARTICLE Method. *Mol. Phys.* **1992**, *76*, 1319.
(7) Orea, P.; Duda, Y.; Alejandre, J. Oscillatory Surface Tension Due to Finite Size Effects. *J. Chem. Phys.* **2005**, *123*, 114702.
(8) Gonzalez-Melchor, M.; Orea, P.; Lopez-Lemus, J.; Bresme, F.; Alejandre, J. Stress anisotropy induced by periodic boundary conditions. *J. Chem. Phys.* **2005**, *122*, 094503.
(9) Janecek, J. Long Range Corrections in Inhomogeneous Simulations. *J. Phys. Chem. B* **2006**, *110*, 6264–6269.
(10) Lopez-Lemus, J.; Romero-Bastida, M.; Darden, T. A.; Alejandre, J. Liquid-vapour equilibrium of n-alkanes using interface simulations. *Mol. Phys.* **2006**, *104*, 2413–2421.
(11) Shen, V. K.; Mountain, R. D.; Errington, J. R. Comparative Study of the Effect of Tail Corrections on Surface Tension Determined by Molecular Simulation. *J. Phys. Chem. B* **2007**, *111*, 6198–6207.
(12) Ibergay, C.; Ghoufi, A.; Goujon, F.; Ungerer, P.; Boutin, A.; Rousseau, B.; Malfreyt, P. Molecular Simulations of the n-Alkane Liquid Vapor Interface: Interacial Properties and their Long Range Corrections. *Phys. Rev. E* **2007**, *75*, 051602.
(13) Mountain, R. D. An Internally Consistent Method for the Molecular Dynamics Simulation of the Surface Tension: Application to Some TIP4P-Type Models of Water. *J. Phys. Chem. B* **2009**, *113*, 482–486.
(14) MacDowell, L. G.; Blas, F. J. Surface tension of fully flexible Lennard-Jones chains: Role of long-range corrections. *J. Chem. Phys.* **2009**, *131*, 074705.
(15) Allen, M.; Tildesley, D. *Computer Simulation of Liquids*; Clarendon Press: Oxford, 1987.
(16) Mansfield, K. F.; Theodorou, D. N. Atomistic Simulation of a Glassy Polymer Surface. *Macromolecules* **1991**, *24*, 4295–4309.
(17) Mecke, M.; Winkelmann, J.; Fischer, J. Molecular Dynamics Simulations of the Liquid-Vapor Interface: The Lennard-Jones Fluid. *J. Chem. Phys.* **1997**, *107*, 9264–9270.
(18) Guo, M.; Lu, B. C.-Y. Long range corrections to thermodynamic properties of inhomogeneous systems with planar interfaces. *J. Chem. Phys.* **1997**, *106*, 3688–3695.
(19) Rowlinson, J.; Widom, B. *Molecular Theory of Capillarity*; Clarendon: Oxford, 1982.
(20) Irving, J. H.; Kirkwood, J. G. The Statistical Mechanical Theory of Transport Processes. IV. The Equations of Hydrodynamics. *J. Chem. Phys.* **1950**, *18*, 817.
(21) Harasima, A. Molecular Theory of Surface Tension. *Adv. Chem. Phys.* **1958**, *1*, 203–237.
(22) Nijmeijer, M. J. P.; Bruin, C.; Bakker, A. F.; van Leeuwen, J. M. J. Wetting and drying of an inert wall by a fluid in a molecular-dynamics simulation. *Phys. Rev. A* **1990**, *42*, 6052–6059.
(23) Honnell, K. G.; Hall, C. K.; Dickman, R. On the Pressure Equation for Chain Molecules. *J. Chem. Phys.* **1987**, *87*, 664–674.
(24) Müller, M.; MacDowell, L. G. Interface and Surface Properties of Polymer Solutions: Monte Carlo Simulations and Self-Consistent Field Theory. *Macromolecules* **2000**, *33*, 3902–3923.
(25) Gloor, G. J.; Jackson, G.; Blas, F. J.; de Miguel, E. Test Area Simulation Method for the Direct Determination of the Interfacial Tension of Systems with Continuous or Discontinuous Potentials. *J. Chem. Phys.* **2005**, *123*, 134703.
(26) MacDowell, L. G.; Bryk, P. Direct Calculation of Interfacial Tensions from Computer Simulation: Results for Freely Jointed Tangent Hard Sphere Chains. *Phys. Rev. E* **2007**, *75*, 061609.
(27) Blas, F. J.; MacDowell, L. G.; de Miguel, E.; Jackson, G. Vapor-liquid interfacial properties of fully-flexible Lennard-Jones chains. *J. Chem. Phys.* **2008**, *129*, 144703.
(28) Martin, M. G.; Siepmann, J. I. Transferable Potentials for Phase Equilibria. 1. United-Atom Description of n-Alkanes. *J. Phys. Chem. B* **1998**, *102*, 2569–2577.
(29) Jorgensen, W. L.; Madura, J. D.; Swenson, C. J. Optimized Intermolecular Potential Functions for Liquid Hydrocarbons. *J. Am. Chem. Soc.* **1984**, *106*, 6638–6646.
(30) de Miguel, E. Computation of surface tensions using expanded ensemble simulations. *J. Phys. Chem. B* **2008**, *112*, 4674–4679.
(31) Errington, J. R.; Kofke, D. A. Calculation of Surface Tension via Area Sampling. *J. Chem. Phys.* **2007**, *127*, 174709.

(32) Mecke, M.; Winkelmann, J.; Fischer, J. Molecular Dynamics Simulations of the Liquid-Vapor Interface: Binary Mixtures of Lennard-Jones Fluids. *J. Chem. Phys.* **1999**, *110*, 1188–1194.
(33) Janecek, J.; Krienke, H.; Schmeer, G. Interfacial Properties of Cyclic Hydrocarbons: A Monte Carlo Study. *J. Phys. Chem. B* **2006**, *110*, 6916–6923.
(34) Orea, P.; Duda, Y.; Alejandre, J. Surface Tension of a Square Well Fluid. *J. Chem. Phys.* **2003**, *118*, 5635–5639.
(35) Trokhymchuk, A.; Alejandre, J. Computer Simulations of Liquid/Vapor Interfaces in Lennard-Jones Fluids: Some Questions and Answers. *J. Chem. Phys.* **1999**, *111*, 8510–8523.
(36) de Pablo, J. J.; Laso, M.; Suter, U. W. Simulation of Polyethylene above and below the Melting Point. *J. Chem. Phys.* **1992**, *96*, 2395–2403.
(37) Siepmann, J. I.; Frenkel, D. Configurational-Bias Monte Carlo: A New Sampling Scheme for Flexible Chains. *Mol. Phys.* **1992**, *75*, 59–70.
(38) MacDowell, L. G.; Vega, C.; Sanz, E. Equation of State of Model Branched Alkanes: Theoretical Predictions and Configurational Bias Monte Carlo Simulations. *J. Chem. Phys.* **2001**, *115*, 6220–6235.
(39) *NIST Standard Reference Database Number 69*; Linstrom, P., Mallard, W., Eds.; National Institute of Standards and Technology: Gaithersburg, MD, 2010. http://webbook.nist.gov.
(40) Mendoza, F. N.; López-Rendón, R.; López-Lemus, J.; Cruz, J.; Alejandre, J. Surface Tension of Hydrocarbon Chains at the Liquid-Vapour Interface. *Mol. Phys.* **2008**, *106*, 1055–1059.
(41) Baidakov, V. G.; Sulla, I. I. The Surface Tension of Ethane. *Ukr. Fiz. Zh.* **1987**, *32*, 885–887.
(42) Born, M.; Wolf, E. *Principles of optics: electromagnetic theory of propagation, interference and diffraction of light*, 5th ed.; Pergamon Press: Oxford, 1975.

Received for review May 29, 2010. Accepted August 12, 2010. This work was supported by Ministerio de Educacion y Ciencia through project FIS2010-22047-C05-05 and by Comunidad Autonoma de Madrid throught project MODELICO-P2009/ESP-1691.

JE100578Z